NATIONAL ADVISORY COMMITTEE FOR AERONAUTICS

REPORT No. 828

BENDING AND SHEAR STRESSES DEVELOPED BY THE INSTANTANEOUS ARREST OF THE ROOT OF A MOVING CANTILEVER BEAM

By ELBRIDGE Z. STOWELL, EDWARD B. SCHWARTZ, and JOHN C. HOUBOLT

THIS DOCUMENT ON LOAN FROM THE FILES OF

NATIONAL ADVISORY COMMITTEE FOR AERONAUTICS
LANGLEY AERONAUTICAL LABORATORY
LANGLEY FIELD, HAMPTON, VIRGINIA



RETURN TO THE ABOVE ADDRESS.

REQUESTS FOR PUBLICATIONS SHOULD BE ADDRESSED AS FOLLOWS:

NATIONAL ADVISORY COMMITTEE FOR AERONAUTICS 1724 F STREET, N.W., WASHINGTON 25, D.C.

1945

AERONAUTIC SYMBOLS

1. FUNDAMENTAL AND DERIVED UNITS

AXXXX		Metric		English	
	Symbol	Unit	Abbrevia- tion	Unit	Abbrevia- tion
Length Time Force	l t F	metersecondweight of 1 kilogram	m s kg	foot (or mile) second (or hour) weight of 1 pound	ft (or mi) sec (or hr) lb
Power	P	horsepower (metric) /kilometers per hour meters per second	kph	horsepower miles per hour feet per second	hp mph fps

2. GENERAL SYMBOLS

W g m	Weight= mg Standard acceleration of gravity= 9.80665 m/s^2 or 32.1740 ft/sec^2 $Mass=\frac{W}{g}$ Moment of inertia= mk^2 . (Indicate axis of radius of gyration k by proper subscript.) Coefficient of viscosity	 Kinematic viscosity Density (mass per unit volume) Standard density of dry air, 0.12497 kg-m⁻⁴-s² at 15° C and 760 mm; or 0.002378 lb-ft⁻⁴ sec² Specific weight of "standard" air, 1.2255 kg/m³ or 0.07651 lb/cu ft
μ		MIC SYMBOLS
S	Area	iw Angle of setting of wings (relative to thrust line)
Su	Area of wing	i. Angle of stabilizer setting (relative to thrust
G	Gap	line)
b	Span	Q Resultant moment
C	Chord	Ω Resultant angular velocity
A	Aspect ratio, $\frac{b^a}{S}$	R Reynolds number, $\rho \frac{Vl}{\mu}$ where l is a linear dimen-
V	True air speed	sion (e.g., for an airfoil of 1.0 ft chord, 100 mph,
q	Dynamic pressure, $\frac{1}{2} ho V^2$	standard pressure at 15° C, the corresponding Reynolds number is 935,400; or for an airfoil
L	Lift, absolute coefficient $C_{\mathtt{z}} = \frac{L}{qS}$	of 1.0 m chord, 100 mps, the corresponding Reynolds number is 6,865,000)
D	Drag, absolute coefficient $C_D = \frac{D}{qS}$	$lpha$ Angle of attack ϵ Angle of downwash
		Angle of downwash α_{o} Angle of attack, infinite aspect ratio
D_{o}	Profile drag, absolute coefficient $C_{D_0} = \frac{D_0}{qS}$	α_i Angle of attack, induced
D_t	Induced drag, absolute coefficient $C_{D_i} = \frac{D_i}{qS}$	α_a Angle of attack, absolute (measured from zerolift position)
D_{v}	Parasite drag, absolute coefficient $C_{Dp} = \frac{D_p}{qS}$	γ Flight-path angle
C	Cross-wind force, absolute coefficient $C_{\sigma} = \frac{C}{qS}$	

REPORT No. 828

BENDING AND SHEAR STRESSES DEVELOPED BY THE INSTANTANEOUS ARREST OF THE ROOT OF A MOVING CANTILEVER BEAM

By ELBRIDGE Z. STOWELL, EDWARD B. SCHWARTZ, and JOHN C. HOUBOLT

Langley Memorial Aeronautical Laboratory

Langley Field, Va,

National Advisory Committee for Aeronautics

Headquarters, 1500 New Hampshire Avenue NW., Washington 25, D. C.

Created by act of Congress approved March 3, 1915, for the supervision and direction of the scientific study of the problems of flight (U. S. Code, title 49, sec. 241). Its membership was increased to 15 by act approved March 2, 1929. The members are appointed by the President, and serve as such without compensation.

JEROME C. HUNSAKER, Sc. D., Cambridge, Mass., Chairman

Lyman J. Briggs, Ph. D., Vice Chairman, Director, National Bureau of Standards.

Charles G. Abbot, Sc. D., Vice Chairman, Executive Committee, Secretary, Smithsonian Institution.

HENRY H. ARNOLD, General, United States Army, Commanding General, Army Air Forces, War Department.

WILLIAM A. M. BURDEN, Assistant Secretary of Commerce for Aeronautics.

Vannevar Bush, Sc. D., Director, Office of Scientific Research and Development, Washington, D. C.

WILLIAM F. DURAND, Ph. D. Stanford University, California.

OLIVER P. ECHOLS, Major General, United States Army, Chief of Matériel, Maintenance, and Distribution, Army Air Forces, War Department. Aubrey W. Fitch, Vice Admiral, United States Navy, Deputy Chief of Naval Operations (Air), Navy Department.

William Littlewood, M. E., Jackson Heights, Long Island, N. Y.

Francis W. Reichelderfer, Sc. D., Chief, United States Weather Bureau.

LAWRENCE B. RICHARDSON, Rear Admiral, United States Navy, Assistant Chief, Bureau of Aeronautics. Navy Department.

EDWARD WARNER, Sc. D., Civil Aeronautics Board, Washington, D. C.

ORVILLE WRIGHT, Sc. D., Dayton, Ohio.

Theodore P. Wright, Sc. D., Administrator of Civil Aeronautics, Department of Commerce.

George W. Lewis, Sc. D., Director of Aeronautical Research

JOHN F. VICTORY, LL. M., Secretary

Henry J. E. Reid, Sc. D., Engineer-in-Charge, Langley Memorial Aeronautical Laboratory, Langley Field, Va. Smith J. Defrance, B. S., Engineer-in-Charge, Ames Aeronautical Laboratory, Moffett Field, Calif. Edward R. Sharp, Ll. B., Manager, Aircraft Engine Research Laboratory, Cleveland Airport, Cleveland, Ohio Carlton Kemper, B. S., Executive Engineer, Aircraft Engine Research Laboratory, Cleveland Airport, Cleveland, Ohio

TECHNICAL COMMITTEES

AERODYNAMICS

OPERATING PROBLEMS

POWER PLANTS FOR AIRCRAFT

MATERIALS RESEARCH COORDINATION

AIRCRAFT CONSTRUCTION

Coordination of Research Needs of Military and Civil Aviation
Preparation of Research Programs
Allocation of Problems
Prevention of Duplication

Langley Memorial Aeronautical Laboratory
Langley Field, Va.

Ames Aeronautical Laboratory
Moffett Field, Calif.

AIRCRAFT ENGINE RESEARCH LABORATORY, Cleveland Airport, Cleveland, Ohio Conduct, under unified control, for all agencies, of scientific research on the fundamental problems of flight

Office of Aeronautical Intelligence, Washington, D. C.

Collection, classification, compilation, and dissemination of scientific and technical information on aeronautics

REPORT NO. 828

BENDING AND SHEAR STRESSES DEVELOPED BY THE INSTANTANEOUS ARREST OF THE ROOT OF A MOVING CANTILEVER BEAM

By Elbridge Z. Stowell, Edward B. Schwartz, and John C. Houbolt

SUMMARY

A theoretical and experimental investigation has been made of the behavior of a cantilever beam in transverse motion when its root is suddenly brought to rest. Equations are given for determining the stresses, the deflections, and the accelerations that arise in the beam as a result of the impact. The theoretical equations, which have been confirmed experimentally, reveal that, at a given percentage of the distance from root to tip, the bending stresses for a particular mode are independent of the length of the beam whereas the shear stresses vary inversely with the length.

INTRODUCTION

When an airplane lands, the vertical component of the velocity is rapidly reduced to zero. In the absence of a thorough analysis of the stresses that arise from such shocks, it is customary for engineers to assume that the landing loads are static and independent of the elastic properties of the structure. As an initial step in the study of elastic structures under shock loads, an investigation has been made to determine the effect on a simple structure of the sudden arrest of its motion and the effect of the geometry of the structure on the stresses that result. The particular case treated in this report covers the basic problem of the instantaneous arrest of the root of a moving cantilever beam. The solution of this problem gives the energy consumed in exciting the different modes of vibration and the stresses, deflections, and accelerations that result throughout the beam.

This investigation is based on the usual engineering beam theory in which the deflections are considered to be the result of bending alone and shear deflections are neglected. The theory, as applied to ordinary beams, gives reasonably good results as long as the distance between inflection points is greater than a few times the depth of the beam. When this theory for beam action is used in vibration problems, such as the problem in the present paper, the results are satisfactory for those modes of vibration for which the nodes are not too close together. This report summarizes the results of a theoretical solution, given in the appendix, and presents an experimental verification of these results.

SYMBOLS

 $E \qquad \text{modulus of elasticity} \\ \gamma \qquad \text{weight density of material} \\ \lambda \qquad \text{coefficient of equivalent viscous damping of} \\ \alpha \qquad \text{material} \\ c \qquad \text{velocity of sound in material} \left(\sqrt{\frac{Eg}{\gamma}}\right)$

L	length of beam
I	moment of inertia of cross section of beam about
	neutral axis
A	cross-sectional area of beam
ρ	radius of gyration of cross section of beam $\left(\sqrt{\frac{I}{A}}\right)$
\boldsymbol{x}	coordinate along beam measured from root
y	distance from neutral axis of beam to any fiber
t	time, zero at impact
n	operator $\left(\frac{\partial}{\partial x}\right)$

acceleration of gravity

n	integers 1, 2, 3, etc., designating a particular
	mode of vibration
θ_n	<i>n</i> th positive root $1 + \cos \theta \cosh \theta = 0$
ω_n	undamped natural angular frequency of nth mode,

$$\omega_n$$
 undamped natural angular frequency of n th mode, radians per second $\left(
ho c \, rac{ heta_n^{\,\,2}}{L^2}
ight)$

damped natural angular frequency of
$$n$$
th mode, radians per second $\left(\omega_n\sqrt{1-\frac{\lambda^2\omega_n^2}{4E^2}}\right)$ (When $\frac{\lambda^2\omega_n^2}{4E^2}>1$, the "frequency" is defined by $\omega_n'=\omega_n\sqrt{\frac{\lambda^2\omega_n^2}{4E^2}-1}$.)

v	velocity of beam prior to impact
w(x, t)	deflection of beam at station x and time t
$w_n(x, t)$	deflection of beam at station x and time t for
	nth mode of vibration

$$a(x, t)$$
 acceleration of beam at station x and time t acceleration of beam at station x and time t for n th mode of vibration

$\sigma(x, y, t)$	bending stress in beam at station x, distance
	from neutral axis y , and time t
$\sigma_n(x, y, t)$	bending stress in beam at station x , distance
	from neutral exists and time t for ath mode of

$o_n(x, y, v)$	from neutral axis y , and time t for n th mode of
=(a t)	vibration average shear stress over cross section of beam at
$\overline{\tau}(x, t)$	station r and time t

	station x an	d tune	ı				
$\overline{\tau}_n(x,t)$	average shear	stress	over	cross	section	of be	am
	at station	x and	time	t fo	r nth	mode	of
	vibration						*

	11010000
A_n	bending-stress coefficient
B_n	shear-stress coefficient
C	deflection coefficient

RESULTS AND CONCLUSIONS THEORETICAL

When a cantilever beam under uniform translation in a direction perpendicular to its length has it root instantaneously brought to rest, there is excited a theoretically infinite number of modes of vibration. With each successive mode, damping has an increasing influence upon the frequencies and amplitudes of vibration and, for sufficiently high modes, even changes the type of motion from oscillatory to nonoscillatory motion. In the lower modes, however, damping has little effect, and only terms of the first order in damping need to be included in the equations. Only the equations applicable to the lower modes, which alone are of importance in any practical case, are presented in this section of the paper. For a more complete treatment of damping, see the appendix.

The angular frequencies (2π times the frequencies in cps) are given by the equation

$$\omega_n = \rho c \, \frac{\theta_n^2}{L^2} \tag{1}$$

where θ_n has the following values for successive modes of vibration:

$$\begin{array}{lll} \theta_1 \! = \! 1.875104 & \theta_5 \! = \! 14.137168 \\ \theta_2 \! = \! 4.694098 & \theta_6 \! = \! 17.278759 \\ \theta_3 \! = \! 7.854757 & \theta_4 \! = \! 10.995541 & \theta_n \! \approx \! \frac{1}{2} \left(2n \! - \! 1 \right) \! \pi, \; n \! > \! 6 \end{array}$$

The energy that the beam possesses before impact is consumed in exciting the various modes of vibration and is distributed among the modes as follows:

Mode, n	Percentage of energy
1	61.3
3	18. 8 7. 4
5	3. 2 1. 9
6 7 to ∞	1.3 6.1

This distribution of energy among the different modes of vibration is presented graphically in figure 1.

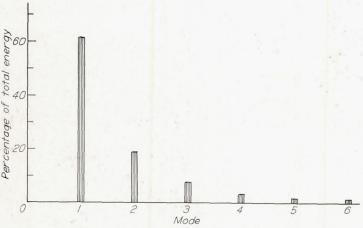


FIGURE 1.—Distribution of energy among the modes of vibration.

All stresses, deflections, and accelerations are damped sinusoidal functions of time and vary along the length of the beam. The bending stress $\sigma_n(x, y, t)$ and the average shear stress $\overline{\tau}_n(x, t)$, associated with the *n*th mode of vibration, are given by the equations

$$\sigma_n(x, y, t) = A_n \frac{v}{c} \frac{y}{\rho} E e^{-\frac{\lambda \omega_n^2}{2E}t} \sin \omega_n t$$
 (2)

$$\overline{\tau}_{n}(x,t) = B_{n} \frac{v}{c} \frac{\rho}{L} E e^{-\frac{\lambda \omega_{n}^{2}}{2E}t} \sin \omega_{n} t$$
(3)

The variation of the dimensionless coefficients A_n and B_n with x/L is given for n=1, 2, and 3 in figures 2 and 3. The

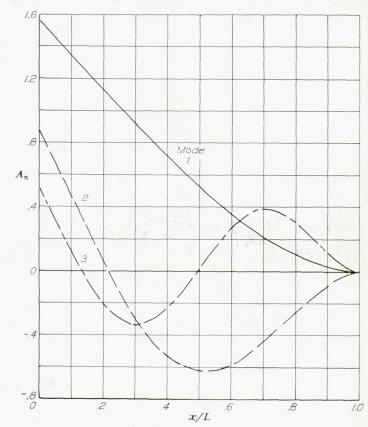


FIGURE 2.—Variation of bending-stress coefficient A_n with x/L.

highest values of A_n and B_n , and hence the highest stresses, occur at the root of the beam. These values, for the first six modes, are

Mode, n	A _n at root	B_n at root
1	1. 566	2.146
2 3	. 868	4. 149 3. 994
4 5	. 364	4. 00 4. 00
6	. 231	4.00

The foregoing values of A_n and B_n at the root are presented graphically in figure 4.

The maximum values with respect to time of $\sigma_n(x, y, t)$ and $\overline{\tau}_n(x, t)$ associated with the *n*th mode of vibration, when the effects of damping are neglected, are

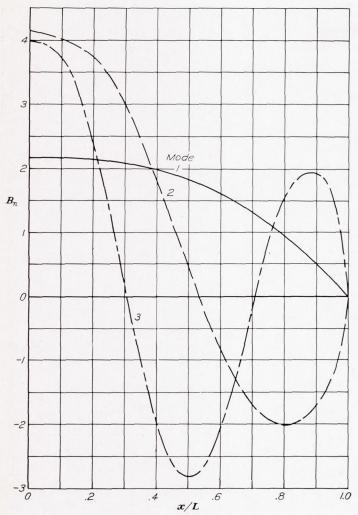


FIGURE 3.—Variation of shear-stress coefficient B_n with x/L.

$$\sigma_n(x, y) = A_n \frac{v}{c} \frac{y}{\rho} E \tag{4}$$

$$\overline{\tau}_n(x) = B_n \frac{v}{c} \frac{\rho}{L} E \tag{5}$$

The deflections $w_n(x, t)$ for the *n*th mode of vibration are given by the equation

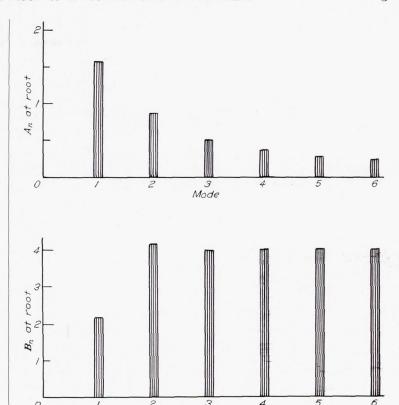
$$w_n(x,t) = C_n \frac{v}{c} \frac{L^2}{\rho} e^{-\frac{\lambda \omega_n^2}{2E}t} \sin \omega_n t$$
 (6)

The accelerations $a_n(x, t)$ for the *n*th mode, when damping is sufficiently small, are given by

$$a_n(x, t) = -\omega_n^2 w_n(x, t) \tag{7}$$

The variation of the dimensionless coefficient C_n with x/L is given for n=1, 2, and 3 in figure 5.

The equations (4) to (7) for stress, deflection, and acceleration give the values associated with the *n*th mode of vibration. Since all modes of vibration occur simultaneously, the net results are the superposition of the effects of all modes. This superposition gives the following equations:



 $\label{eq:mode} {\it Mode}$ Figure 4.—Values of bending-stress coefficient A_n and shear-stress coefficient B_n at root.

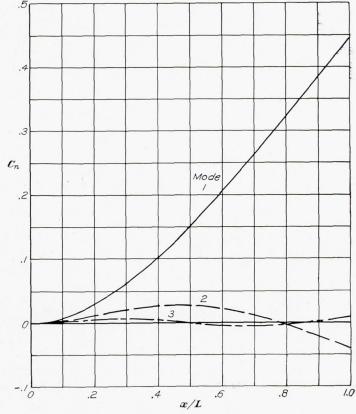


Figure 5.—Variation of deflection coefficient C_n with x/L.

For bending stress,

$$\sigma(x, y, t) = \frac{v}{c} \frac{y}{\rho} E\left(A_1 e^{-\frac{\lambda \omega_1^2}{2E}t} \sin w_1 t + A_2 e^{-\frac{\lambda \omega_2^2}{2E}t} \sin \omega_2 t + \dots\right)$$
(8)

For average shear stress,

$$\tau(x,t) = \frac{v}{c} \frac{\rho}{L} E \left(B_1 e^{-\frac{\lambda \omega_1^2}{2E}t} \sin \omega_1 t + B_2 e^{-\frac{\lambda \omega_2^2}{2E}t} \sin \omega_2 t + \dots \right)$$
(9)

For deflection

$$w(x,t) = \frac{r}{c} \frac{L^2}{\rho} \left(C_1 e^{-\frac{\lambda \omega_1^2}{2E}t} \sin \omega_1 t + C_2 e^{-\frac{\lambda \omega_2^2}{2E}t} \sin \omega_2 t + \dots \right)$$
(10)

For acceleration, when damping is sufficiently small,

$$a(x,t) = \frac{v}{c} \frac{L^2}{\rho} \left(C_1 \omega_1^2 e^{-\frac{\lambda \omega_1^2}{2E}t} \sin \omega_1 t + C_2 \omega_2^2 e^{-\frac{\lambda \omega_2^2}{2E}t} \sin \omega_2 t + \dots \right)$$
(11)

The equation for bending stress (equation (4)) reveals that, at a given percentage of the distance from root to tip, the bending stress for a particular mode is independent of the length of the beam and depends only on the velocity before impact. The equation for shear stress (equation (5)) reveals that the shear stresses at any station vary inversely with the length of the beam. These results are contrary to those that might be expected on the basis of experience with the static behavior of structures. For this reason an experimental investigation was made.

EXPERIMENTAL

A circular steel tube of 1-inch outside diameter and 0.028-inch wall thickness was mounted symmetrically on the end of a pendulum to form a pair of cantilever beams. (See fig. 6.) The pendulum was permitted to start its swing from a predetermined position and was suddenly brought to rest at the bottom of its swing against an electromagnet used to prevent rebound. The effect of length was studied by reducing the length of the tube in successive tests. The bending and shear strains were measured by electrical strain gages that were mounted on the tube as shown in figure 7. Each pair of gages was incorporated into a Wheatstone bridge circuit as shown diagrammatically in figure 8. The outputs of the bridge systems were fed through a strain-gage

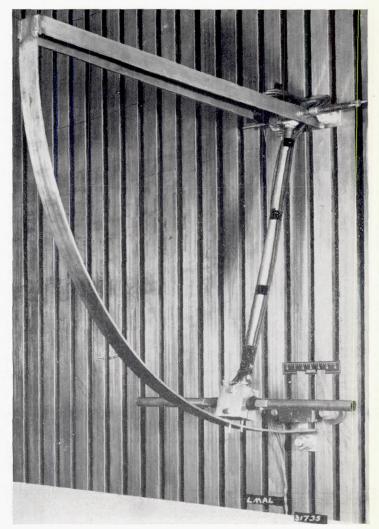


FIGURE 6.—Pendulum assembly used in impact test.

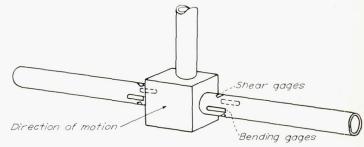


FIGURE 7.—Location of strain gages on tube.

amplifier into a multichannel oscillograph that recorded the strains on moving photographic paper. The amplitude of the components of strain due to the modes of higher frequency was reduced, however, because of the response characteristics of the oscillograph. The frequency-response curve for the oscillograph used is given in figure 9.

Typical records for tubes of two lengths are shown in figure 10. Inspection of the record for the cantilever beam

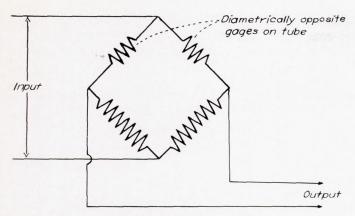


FIGURE 8.—Bridge circuit used in tests.

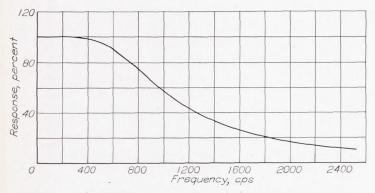
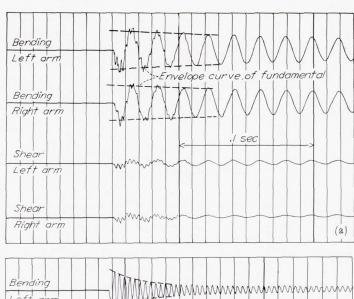


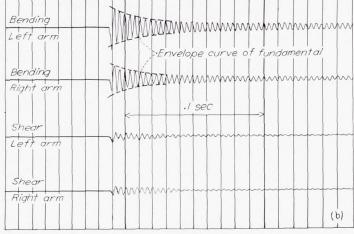
FIGURE 9.—Frequency response of strain-gage amplifier and Miller (2000~) oscillograph; 0.69 critical damping.

26¾ inches long shows the superposition of the second and third modes upon the first mode. The record shows that, in the case of the bending strain, the contribution of the second mode is small; whereas, in the case of the shear strain, the contribution of the second mode is large. This observation confirms qualitatively the theoretical results shown in figure 4. The same effect is not shown, however, in the record for the cantilever beam 11¾ inches long because of the combined action of damping and reduced response of the oscillograph to the higher frequencies associated with this short length of tube.

The bending stresses computed by use of equation (8), in which only the first three modes are used, are given by the solid-line curve of figure 11 for the cantilever beam 26% inches long. Comparison of this curve with the record obtained during the first ½ cycle of the first mode (see fig. 10) shows good agreement as regards the wave shape.

Because of the damping present in the tube and the response characteristics of the oscillograph, the only component of vibration that could be satisfactorily recorded for all lengths of cantilever tube was the fundamental or first mode. The quantitative results of the tests consequently were based upon this mode of vibration. This procedure is sound because the effects of the various harmonics are independent of one another. In the analysis of the results, the data had to be corrected for the influence of the magnet.





(a) Cantilever length, 2634 inches.

FIGURE 10.—Portions of typical records obtained for two different lengths of tube.

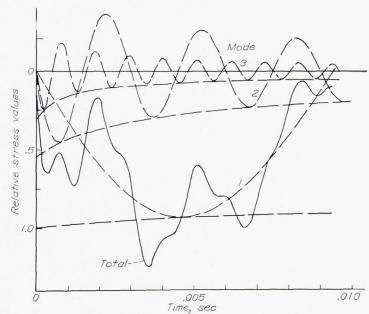


FIGURE 11.—Theoretical wave form for extreme-fiber bending stress at root obtained from the first three modes of vibration. Steel tube, 1-inch outside diameter; wall thickness, 9.028 inch; length, 2634 inches.

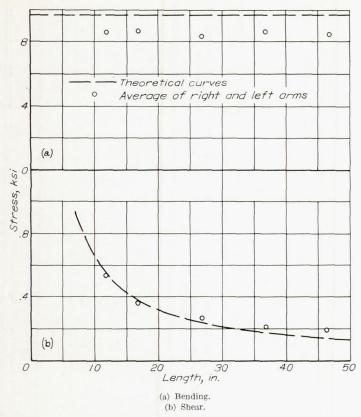


FIGURE 12.—Comparison of experimentally and theoretically determined maximum stresses of fundamental mode at root of cantilever tube. Impact velocity, 2.5 feet per second.

The observed frequencies are compared with the frequencies computed from equation (1) for the first mode in the following table:

	Frequency			
Length (in.)	Observed (cps)	Computed (cps)		
46¾ 36¾	17. 5 27. 9	17. 5 28. 2		
26¾ 16¾	52. 1 131	53. 2 137		
1134	272	277		

The experimental values of extreme-fiber bending stresses and the shear stresses at the root, for the fundamental mode, are plotted in figure 12. In figure 12 are also shown the corresponding theoretical curves of equation (4) for bending and equation (5) for shear with n taken as 1. It is observed that the experimental points follow the trend of and lie close to the theoretical curves.

Langley Memorial Aeronautical Laboratory, National Advisory Committee for Aeronautics, Langley Field, Va., September 27, 1944.

APPENDIX

THEORETICAL DERIVATION

General analysis.—Consider a beam of uniform cross section in equilibrium. If a portion of the beam is suddenly disturbed, as by a shock, in a direction perpendicular to its length, the beam is set into damped bending oscillations. The equation of motion for these bending oscillations is given by the differential equation (reference 1)

$$E\rho^2 \frac{\partial^4 w}{\partial x^4} + \lambda \rho^2 \frac{\partial^5 w}{\partial x^4 \partial t} + \frac{\gamma}{g} \frac{\partial^2 w}{\partial t^2} = 0$$
 (A1)

The damping term $\lambda \rho^2 \frac{\partial^5 w}{\partial x^4 \partial t}$ is derived on the assumption that the longitudinal damping force per unit area at any point on the cross section of the beam is proportional to the rate of change of longitudinal strain at that point. (See reference 2.) This type of force is analogous to ordinary viscous drag, in which the tangential force per unit area is proportional to the rate of change of shear strain. With the use of the notation $c^2 = \frac{Eg}{\gamma}$, equation (A1) can be written

$$\frac{\partial^4 w}{\partial x^4} + \frac{\lambda}{E} \frac{\partial^5 w}{\partial x^4 \partial t} + \frac{1}{c^2 \rho^2} \frac{\partial^2 w}{\partial t^2} = 0 \tag{A2}$$

In accordance with the Heaviside operational methods (reference 3), equation (A2) may be reduced to an ordinary differential equation of the fourth order by writing $p = \frac{\delta}{\delta t}$; thus,

$$\left(1+p\frac{\lambda}{E}\right)\frac{d^4w}{dx^4} + \frac{p^2}{c^2o^2}w = 0$$
 (A3)

The general solution of equation (A3) is

$$w = P \cosh \theta \frac{x}{L} + Q \sinh \theta \frac{x}{L} + R \sin \theta \frac{x}{L} + S \cos \theta \frac{x}{L}$$
 (A4)

where

$$\theta = L \sqrt{\frac{ip}{\rho c \sqrt{1 + p \frac{\lambda}{E}}}}$$

The coefficients P, Q, R, and S are to be determined from the boundary conditions. The case under consideration is that of a cantilever moving with uniform velocity v and having its base brought instantaneously to rest. The boundary conditions for this case are

$$\left(\frac{\partial w}{\partial t}\right)_{x=0} = p (w)_{x=0} = v - v\mathbf{1}$$

$$\left(\frac{\partial w}{\partial x}\right)_{x=0} = \left(\frac{\partial^2 w}{\partial x^2}\right)_{x=L} = \left(\frac{\partial^3 w}{\partial x^3}\right)_{x=L} = 0$$

The velocity of the root as given by the first boundary condition is represented graphically in figure 13(a). The rules of the Heaviside calculus, however, have been devised for a disturbance, called the unit function 1, shown in figure 13(b). By the principle of superposition, the velocity function shown in figure 13(a) may be considered as a superposition of those shown in figures 13(c) and 13(d). The velocity therefore consists of a constant velocity v (fig. 13(c)) added to the solution of the problem obtained by the Heaviside expansion theorem for the disturbance shown in figure 13(d). On the basis of this procedure, the first boundary

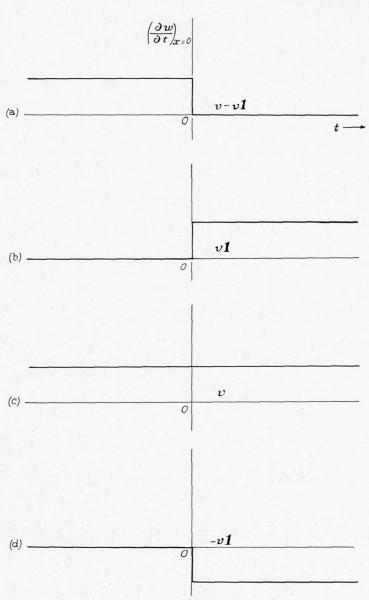


FIGURE 13.—Graphic representation of various velocity functions.

condition may be written

$$\left(\frac{\partial w}{\partial t}\right)_{x=0} = p (w)_{x=0} = -v\mathbf{1}$$

With the application of the boundary conditions to equation (A4), the operational form of the solution for the velocity (that induced by the disturbance) is found to be

$$pw = \frac{-v\mathbf{I}}{2(1+\cosh\theta\cos\theta)} \left[(1+\cos\theta\cosh\theta) \left(\cosh\theta\frac{x}{L} + \cos\theta\frac{x}{L}\right) + \sin\theta\sinh\theta \left(\cosh\theta\frac{x}{L} - \cos\theta\frac{x}{L}\right) + (\sinh\theta\cos\theta + \cosh\theta\sin\theta) \left(\sin\theta\frac{x}{L} - \sinh\theta\frac{x}{L}\right) \right]$$
(A5)

Interpretation of this operational expression and addition of the constant velocity v gives for the total velocity

$$\frac{\partial w(x,t)}{\partial t} = v - v\mathbf{I} + 2v\sum_{n=1}^{\infty} F\left(\theta_n \frac{x}{L}\right) e^{-\frac{\lambda \omega_n^2}{2E}t} \left[\cos \omega_n' t - \frac{\frac{\lambda \omega_n}{2E}}{\sqrt{1 - \frac{\lambda^2 \omega_n^2}{4E^2}}} \sin \omega_n' t\right] \mathbf{I}$$
(A6)

where

 θ_n nth positive root of $1 + \cos \theta \cosh \theta = 0$

 $\omega_n = \rho c \frac{\theta_n^2}{L^2}$ undamped natural angular frequency of *n*th mode, radians/sec

 $\omega_n' = \omega_n \sqrt{1 - \frac{\lambda^2 \omega_n^2}{4E^2}}$ damped natural angular frequency of nth mode, radians/sec

$$F\left(\theta_{n}\frac{x}{L}\right) = \frac{\sin \theta_{n} \sinh \theta_{n} \left(\cosh \theta_{n}\frac{x}{L} - \cos \theta_{n}\frac{x}{L}\right) - \left(\cosh \theta_{n} \sin \theta_{n} + \sinh \theta_{n} \cos \theta_{n}\right) \left(\sinh \theta_{n}\frac{x}{L} - \sin \theta_{n}\frac{x}{L}\right)}{\theta_{n} \left(\cosh \theta_{n} \sin \theta_{n} - \sinh \theta_{n} \cos \theta_{n}\right)}$$

Integration of equation (A6) with respect to the time with the condition $(w)_{t=0}=0$ gives for the deflection

$$w(x,t) = 2v \sum_{n=1}^{\infty} \frac{F\left(\theta_n \frac{x}{L}\right)}{\omega_n'} e^{-\frac{\lambda \omega_n^2}{2E}t} \sin \omega_n' t \mathbf{I}$$

$$= \frac{v}{c} \frac{L^2}{\rho} \sum_{n=1}^{\infty} C_n \frac{1}{\sqrt{1 - \frac{\lambda^2 \omega_n^2}{4E^2}}} e^{-\frac{\lambda \omega_n^2}{2E}t} \sin \omega_n' t \mathbf{I} \qquad (A7)$$

where

$$C_n = \frac{2F\left(\theta_n \frac{x}{L}\right)}{\theta_n^2}$$

The contribution of the *n*th mode to the deflection is

$$w_n(x,t) = \frac{v}{c} \frac{L^2}{\rho} C_n \frac{1}{\sqrt{1 - \frac{\lambda^2 \omega_n^2}{4E^2}}} e^{-\frac{\lambda \omega_n^2}{2E}t} \sin \omega_n' t \mathbf{1}$$
 (A8)

When $\frac{\lambda \omega_n}{2E} > 1$, equation (A8) may be put in the form

$$w_n(x, t) = \frac{v}{c} \frac{L^2}{\rho} C_n \frac{1}{\sqrt{\frac{\lambda^2 \omega_n^2}{4E^2} - 1}} e^{-\frac{\lambda \omega_n^2}{2E}t} \sinh \omega_n' t \mathbf{1}$$
 (A9)

where now

$$\omega_n' = \omega_n \sqrt{\frac{\lambda^2 \omega_n^2}{4E^2} - 1}$$

The form indicated by equation (A8), where $\frac{\lambda \omega_n}{2E} < 1$, is characteristic of the lower modes and represents damped oscillatory motion. The form indicated by equation (A9), where $\frac{\lambda \omega_n}{2E} > 1$ (damping greater than critical), is characteristic of the higher modes and represents subsidence motion.

From equation (A6) for velocity and equation (A7) for deflection, the complete behavior of the cantilever may be determined. The quantities of interest are the bending stresses, the shear stresses, and to some extent the accelerations. When damping is present, the equations representing the contribution of the nth mode to these quantities may be given in the two forms indicated by equations (A8) and (A9). In subsequent equations, however, only the form indicated by equation (A8) is given because it is characteristic of the modes that are of practical importance.

Bending stresses.—The bending stresses $\sigma(x, y, t)$ at any fiber distance y from the neutral axis are

$$\sigma(x, y, t) = Ey \frac{\partial^{s} w}{\partial x^{s}}$$

$$= E \frac{v}{c} \frac{y}{\rho} \sum_{n=1}^{\infty} A_{n} \frac{1}{\sqrt{1 - \frac{\lambda^{2} \omega_{n}^{2}}{4E^{2}}}} e^{-\frac{\lambda \omega_{n}^{2}}{2E}t} \sin \omega_{n}' t \mathbf{1}$$

where

$$A_{n}=2\frac{\sin\theta_{n} \sinh\theta_{n} \left(\cosh\theta_{n} \frac{x}{L} + \cos\theta_{n} \frac{x}{L}\right) - \left(\cosh\theta_{n} \sin\theta_{n} + \sinh\theta_{n} \cos\theta_{n}\right) \left(\sinh\theta_{n} \frac{x}{L} + \sin\theta_{n} \frac{x}{L}\right)}{\theta_{n} \left(\cosh\theta_{n} \sin\theta_{n} - \sinh\theta_{n} \cos\theta_{n}\right)}$$

The bending stress due to only the nth mode is

$$\sigma_n(x, y, t) = E \frac{v}{c} \frac{y}{\rho} A_n \frac{1}{\sqrt{1 - \frac{\lambda^2 \omega_n^2}{4E^2}}} e^{-\frac{\lambda \omega_n^2}{2E}t} \sin \omega_n' t \mathbf{1}$$

Shear stresses.—The average shear stress over the cross section $\bar{\tau}(x,t)$ is

$$\bar{\tau} (x, t) = E\rho^2 \frac{\partial^3 w}{\partial x^3}$$

$$= E \frac{v}{c} \frac{\rho}{L} \sum_{n=1}^{\infty} B_n \frac{1}{\sqrt{1 - \frac{\lambda^2 \omega_n^2}{4E^2}}} e^{-\frac{\lambda \omega_n^2}{2E}t} \sin \omega_n' t \mathbf{1}$$

where

$$B_{n}=2\frac{\sin\theta_{n} \sinh\theta_{n}\left(\sinh\theta_{n}\frac{x}{L}-\sin\theta_{n}\frac{x}{L}\right)-\left(\cosh\theta_{n} \sin\theta_{n}+\sinh\theta_{n} \cos\theta_{n}\right)\left(\cosh\theta_{n}\frac{x}{L}+\cos\theta_{n}\frac{x}{L}\right)}{\cosh\theta_{n} \sin\theta_{n}-\sinh\theta_{n} \cos\theta_{n}}$$

The average shear stress due to only the nth mode is

$$\overline{\tau}_{n}(x, t) = E \frac{v}{c} \frac{\rho}{L} B_{n} \frac{1}{\sqrt{1 - \frac{\lambda^{2} \omega_{n}^{2}}{4E^{2}}}} e^{-\frac{\lambda \omega_{n}^{2}}{2E}t} \sin \omega_{n}' t \mathbf{1}$$

Accelerations.—From equation (A6), with the aid of the relation

$$pF(t) \mathbf{1} = F(0)p\mathbf{1} + F'(t) \mathbf{1}$$

the acceleration anywhere on the beam is found to be

$$a(x,t) = \frac{\partial^2 w(x,t)}{\partial t^2} = \left[2\sum_{n=1}^{\infty} F\left(\theta_n \frac{x}{L}\right) - 1 \right] vp \mathbf{1} - \frac{v}{c} \frac{L^2}{\rho} \sum_{n=1}^{\infty} C_n \frac{\omega_n^2 \left(1 - \frac{\lambda^2 \omega_n^2}{2E^2}\right)}{\sqrt{1 - \frac{\lambda^2 \omega_n^2}{4E^2}}} e^{-\frac{\lambda \omega_n^2}{2E}t} \left(\sin \omega_n' t + \frac{\frac{\lambda \omega_n}{E} \sqrt{1 - \frac{\lambda^2 \omega_n^2}{4E^2}}}{1 - \frac{\lambda^2 \omega_n^2}{2E^2}} \cos \omega_n' t \right) \mathbf{1}$$

With the aid of the orthogonal properties of the functions $F\left(\theta_n \frac{x}{L}\right)$ it is possible to show that the quantity $2\sum_{n=1}^{\infty} F\left(\theta_n \frac{x}{L}\right) - 1$ reduces to zero when $0 < \frac{x}{L} \le 1$. At $\frac{x}{L} = 0$, the quantity $2\sum_{n=1}^{\infty} F\left(\theta_n \frac{x}{L}\right)$ equals zero, and only the term $-vp\mathbf{1}$ remains. This term indicates that at t = 0 an infinite acceleration of zero duration exists at the root.

The acceleration due to only the nth mode is

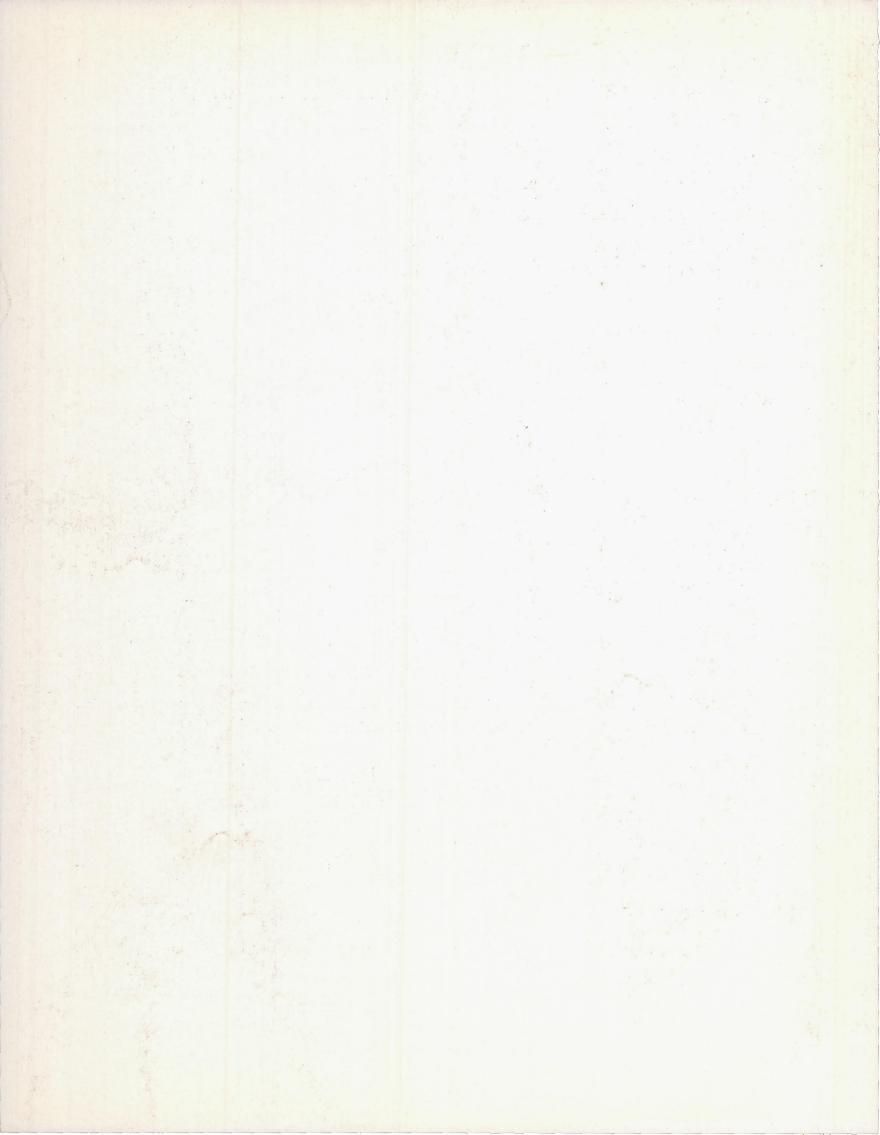
$$a_{n}(x, t) = -\frac{v}{c} \frac{L^{2}}{\rho} \omega_{n^{2}} C_{n} \frac{1 - \frac{\lambda^{2} \omega_{n}^{2}}{2E^{2}}}{\sqrt{1 - \frac{\lambda^{2} \omega_{n}^{2}}{4E^{2}}}} e^{-\frac{\lambda \omega_{n}^{2}}{2E}t} \left[\sin \omega_{n}' t + \frac{\frac{\lambda \omega_{n}}{E} \sqrt{1 - \frac{\lambda^{2} \omega_{n}^{2}}{4E^{2}}}}{1 - \frac{\lambda^{2} \omega_{n}^{2}}{2E^{2}}} \cos \omega_{n}' t \right] \mathbf{1}$$

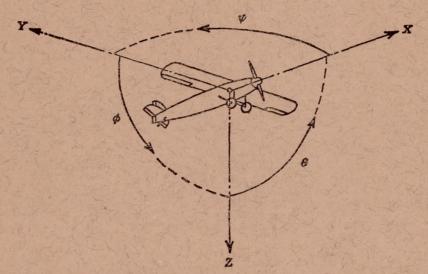
Comparison with the expression for $w_n(x,t)$ (equation (A8)) shows that the acceleration for each mode is out of phase with the deflection. When damping is sufficiently small, however, the relation between the acceleration and the deflection reduces to the well-known result for undamped vibration

$$a_n(x, t) = -\omega_n^2 w_n(x, t)$$

REFERENCES

- Den Hartog, J. P.: Mechanical Vibrations. Second ed., McGraw-Hill Book Co., Inc., 1940, p. 180.
- Honda, Kôtarô, and Konno, Seibei: On the Determination of the Coefficient of Normal Viscosity of Metals. Phil. Mag., ser. 6, vol. 42, no. 247, July 1921, pp. 115–123.
- Carson, John R.: Electric Circuit Theory and the Operational Calculus. McGraw-Hill Book Co., Inc., 1926.





Positive directions of axes and angles (forces and moments) are shown by arrows

1	Axis			Moment about axis			Angle		Velocities	
To the state of th	Designation	Sym- bol	Force (parallel to axis) symbol	Designation	Sym- bol	Positive direction	Designa- tion	Sym- bol	Linear (compo- nent along axis)	Angular
	Longitudinal Lateral Normal	X Y Z	X Y Z	Rolling Pitching Yawing	L M N	$\begin{array}{c} Y \longrightarrow Z \\ Z \longrightarrow X \\ X \longrightarrow Y \end{array}$	Roll Pitch Yaw	φ θ Ψ	u v w	p q r

Absolute coefficients of moment

 $C_{l} = \frac{L}{qbS}$ (rolling)

 $C_m = \frac{M}{qcS}$ (pitching)

 $C_n = \frac{N}{qbS}$ (yawing)

Angle of set of control surface (relative to neutral position), δ. (Indicate surface by proper subscript.)

4. PROPELLER SYMBOLS

D Diameter

p Geometric pitch

p/D Pitch ratio

V' Inflow velocity

V_s Slipstream velocity

T Thrust, absolute coefficient $C_T = \frac{T}{\rho n^2 D^4}$

Q Torque, absolute coefficient $C_Q = \frac{Q}{\rho n^2 D^5}$

P Power, absolute coefficient $C_P = \frac{P}{\rho n^3 D^6}$

 $C_{m{s}}$ Speed-power coefficient $=\sqrt[5]{rac{
ho V^5}{Pn^2}}$

η Efficiency

n Revolutions per second, rps

 $\Phi \qquad \text{Effective helix angle} = \tan^{-1} \left(\frac{V}{2\pi rn} \right)$

5. NUMERICAL RELATIONS

1 hp = 76.04 kg-m/s = 550 ft-lb/sec

1 metric horsepower=0.9863 hp

1 mph=0.4470 mps

1 mps=2.2369 mph

1 lb=0.4536 kg

1 kg=2.2046 lb

1 mi = 1,609.35 m = 5,280 ft

1 m = 3.2808 ft

